11th World Congress on Computational Mechanics (WCCM XI)
5th European Conference on Computational Mechanics (ECCM V)
6th European Conference on Computational Fluid Dynamics (ECFD VI)
E. Oñate, J. Oliver and A. Huerta (Eds)

APPLICATION OF EARSM TURBULENCE MODEL TO SIMULATION OF REACTING FLOW FIELD IN JETIS COMBUSTION CHAMBER

V. BETAK, J. KUBATA AND J. TUMA

Aerospace Research and Test Establishment
Department of Engines
Beranovych 130, 19905 Praha-Letnany, Czech Republic
e-mail: betak@vzlu.cz, www.vzlu.cz

Key Words: *Reacting flow field, RANS turbulence model, EARSM*

Abstract. This paper is interested in the mathematical modeling and approximation of the reacting turbulent flow field with strong anisotropy in a JETIS combustion chamber. Turbulent models based on Boussinesq eddy viscosity assumption or Large Edgy Simulation are traditionally employed for the solution of these types of flows. Linear eddy viscosity model and the assumption of isotropic Reynolds stress tensor are typically used in many industrial cases. This leads to certain limitations such as lower accuracy if model of turbulence is based on Boussinesq assumption or higher time consumption in the case of LES model. Therefore the effect of Explicit Algebraic Reynolds Stress Model (EARSM) is study in this paper. This model is based on two equations k - omega turbulence model with the nonlinear eddy viscosity model and explicit terms for anisotropic parts of the Reynolds stress tensor with computational requirements similar to the standard k - omega model. The EARSM turbulent model is validated via comparison with other turbulent models and public experimental data.

1 INTRODUCTION

CFD methods are recently used in many applications. They are useful especially in cases where is not a direct access for measurement tools or physical conditions are not suitable such as in the combustion chamber of small jet engines with performance up to 100kW [1]. These methods help us to understand and to optimize flow properties inside the chamber or to explain experimental data.

Many researcher activities have shown that modeling of combustion is closed connect to turbulence modeling(e.g. [2]). Therefore a suitable turbulence model must be chosen. The Large Edgy Simulation (LES) models are suitable if we want to obtain detailed solution. These models have a high computational cost due the mesh requirements. If we accept lower accuracy then Reynolds Averaged Navier-Stokes (RANS) can be chosen. These models provide sufficient accuracy for number of industrial cases and their computational demands are acceptable.

RANS models are based on Boussinesq assumption (1) which implies isotropy in Reynolds Stresses. This assumption is not correct in the case of complex flow field. Full Reynolds Stress model should be used but there are not strong benefits (increasing of computational time, lower stability with high order discretization schemes)

$$-\rho\overline{u_i' u_j'} = \mu_t\left(\frac{\partial u_i}{\partial x_j} + \frac{\partial u_j}{\partial x_i}\right) - \frac{2}{3}k\rho\delta_{ij} \quad , \tag{1}$$

Therefore several authors e.g. [3,4,5] use an additional terms for modeling anisotropy part of Reynolds stresses approximation.

This paper deals with application of two-equation turbulence model with the anisotropy term to their calibration for the case of reacting flow field and simulation of the reacting flow field inside combustion chamber based on JeT Induced Swirl (JETIS) where strong anisotropy generated by jets that induced the swirl and by mixing of hot air from the primary zone with the cooling air. Results are compared to earlier data obtained by simpler RANS model.

2 GOVERNING EQUATIONS

Reactive turbulent flow in combustion chamber is modeled by Favre Average Navier-Stokes system of equation in $\Omega \subset \mathbb{R}^3$ described by following system of equations

$$\frac{\partial \rho}{\partial t} + \frac{\partial}{\partial x_i}(\rho u_i) = S_\rho \quad , \tag{2}$$

$$\frac{\partial}{\partial t}(\rho u_i) + \frac{\partial}{\partial x_j}(\rho u_i u_j) = -\frac{\partial \tilde{p}}{\partial x_i} + + \frac{\partial}{\partial x_j}\left[\mu_{eff}\left(\frac{\partial u_i}{\partial x_j} + \frac{\partial u_j}{\partial x_i}\right) - \rho k\left(\frac{2}{3}\delta_{ij} + a_{ij}^{(ex)}\right)\right] + f_i \quad , \tag{3}$$

$$\frac{\partial h}{\partial t} + \frac{\partial}{\partial x_j}(h u_j) = \frac{Dp}{Dt} + \frac{\partial}{\partial x_j}\left[\left(\alpha + \frac{\mu_t}{Pr_t}\right)\frac{\partial h}{\partial x_j}\right] + s_h \quad , \tag{4}$$

where u_i are the components of the mean velocity vector, $\tilde{p}$ is the pressure, $\mu_{eff} = \mu + \mu_t$ is the sum of the kinematic and the turbulent viscosity, k represents the turbulent kinetic energy, $a_{ij}^{(ex)}$ is the anisotropic stress tensor, h is enthalpy, α coefficient of heat diffusion and Pr_t is turbulent Prandtl number S_h, S_ρ and f_i represents source terms in equations.

This system must be supplemented by equations describing transfer of mass fraction Y_i where S_i^Y represent source term of mass fraction.

$$\frac{\partial}{\partial t}(\rho Y_i) + \frac{\partial}{\partial x_j}(\rho Y_i u_j) = \frac{\partial}{\partial x_j}\left[(\mu + \mu_t)\frac{\partial Y_i}{\partial x_j}\right] + s_i^Y \quad . \tag{5}$$

There are additional ODE equations in the system describes droplets motion, evaporation [6] and chemical kinetics[1,6].

The Explicit Algebraic Reynolds Stress Model (EARSM)[5] developed by Hellsten model was used. This model is based on the two-equation $k-\omega$ *SST*

$$\frac{\partial}{\partial t}(k\rho)+\frac{\partial k\rho u_j}{\partial x_j}=P_k-\rho\beta^* k\omega+\frac{\partial}{\partial x_j}\left[(\mu+\mu_t\sigma_k)\frac{\partial k}{\partial x_j}\right] \quad . \tag{6}$$

$$\frac{\partial}{\partial t}(\omega\rho)+\frac{\partial\omega\rho u_j}{\partial x_j}=\gamma\frac{\omega}{k}P_k-\rho\beta\omega^2\frac{\partial}{\partial x_j}\left[(\mu+\mu_t\sigma_\omega)\frac{\partial\omega}{\partial x_j}\right]+\rho\frac{\sigma_d}{\omega}max\left(\frac{\partial k}{\partial x_j}\frac{\partial\omega}{\partial x_j},0\right) \tag{7}$$

$$\mu_t=-\frac{1}{2}\rho(\beta_1+II_\Omega)\beta_6 \quad . \tag{8}$$

$$\begin{aligned} a_{ij}^{(ex)}=&\beta_3\left(\Omega_{ik}\Omega_{kj}-\frac{1}{3}II_\Omega\delta_{ij}\right)+\beta_4\left(S_{ik}\Omega_{kj}-\Omega_{ik}S_{kj}\right)\\ &+\beta_6\left(S_{ik}\Omega_{kl}\Omega_{lj}+\Omega_{ik}\Omega_{kl}S_{lj}-II_\Omega S_{ij}-\frac{2}{3}IV\delta_{ij}\right)\\ &+\beta_9\left(\Omega_{ik}S_{kl}\Omega_{lm}\Omega_{mj}+\Omega_{ik}\Omega_{kl}S_{lm}\Omega_{mj}\right) \end{aligned} \quad . \tag{9}$$

where ω is the rate of specific dissipation, S represent the strain rate tensor and Ω is the vorticity tensor which contain the extra vorticity part

$$\Omega_{ij}=\frac{1}{2}\tau\left(\frac{\partial u_i}{\partial x_j}-\frac{\partial u_j}{\partial x_i}\right)-\frac{\tau}{A_0}\Omega_{ij}^{(r)} \tag{10}$$

where

$$\Omega_{ij}^{(r)}=-e_{ijk}\frac{II_S^2\delta_{km}+12III_S S_{km}+6II_S S_{kl}S_{lm}}{2II_S^3-12III_S^2}S_{pr}\dot{S}_{rq}e_{pqm} \quad . \tag{11}$$

The $\dot{S}$ is a time derivation of strain rate tensor, II_S, III_S, II_Ω, IV are the invariants of the strain rate and vorticity tensors.

The timescale τ is defined as

$$\tau=max\left(\frac{1}{\beta^*\omega},\ 6.0\sqrt{\frac{\nu}{\beta^* k\omega}}\right) \quad . \tag{12}$$

For more details about this model see [5].

3 RESULTS

3.1 Counter flow flame

In the case of counter flow flame the interaction between two jets(oxidizer, fuel) is simulated as is shown in Figure 1. The position of flame is in the middle of domain but the stagnation plane is shifted to the fuel size.

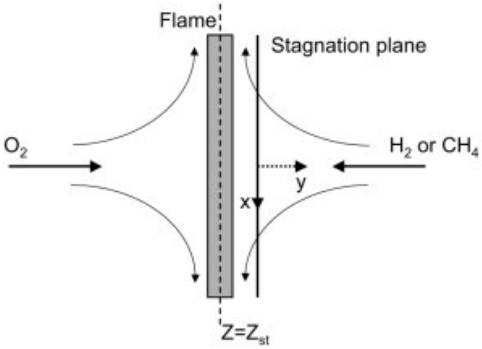

Figure 1: Counter flow flame – Description

This case have been selected for their simplicity and presence of anisotropy in turbulent flow field due the interaction of two contra jets. The first simulation shown huge differences in temperature profiles between isotropy ($k-\epsilon$, $k-\omega\ SST$) and anisotropy (LRR, LES) models as is shown in Figure 2.. One of the chemical timescales that is affected by model of turbulence. This timescale is defined in following form

$$t_k \approx c_{mix}\sqrt{\frac{\mu_t+\mu}{\rho\,\epsilon}} \quad , \tag{13}$$

where c_{mix} represent strength of turbulence reaction. Dissipation of turbulent energy ϵ is in the case of k-epsilon defined as

$$\epsilon \approx \rho\frac{k^2}{\mu_t} \quad , \tag{14}$$

Turbulent kinetic energy k is in general defined as the trace of Reynolds stress tensor $\boldsymbol{R}$

$$k = tr(\boldsymbol{R}) \quad . \tag{15}$$

Therefore the definition of kinetic energy for the case of timescale computation were modified to the following form

$$k = k + tr\left(a_{ij}^{(ex)}\right) \quad . \tag{16}$$

to include the effect of anisotropy tensor. This modification leads to temperature profile similar to temperature profile obtained by LES Smagorinsky model as is shown in Fig 2.

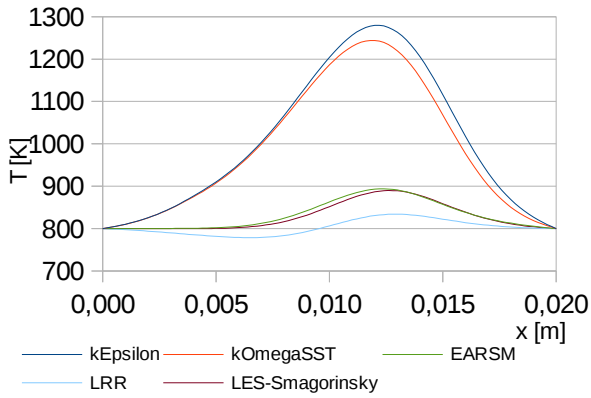

Figure 2: Counter flow flame – Temperature profile for different turbulent models

3.2 Sandia Jet Flames

The case of DLR flames [7] from Sandia database was simulated. The combustion of main fuel jet(42.2 m/s) in co-flow(0.3 m/s) as is shown in Figure 3 is computed in this case.

Figure 3: Sandia test case – Experimental setup

Contours of velocity magnitude are shown in Figure 4. It is evident that the velocity field

of EARMS model corresponds more to reality than the $k-\epsilon$ model.

In figures 5 and 6 are shown comparisons between experimental data and numerical results. In the first case (temperature comparison) is shown good agreement between predicted and measured maximal temperature. The temperature profile is capture better by $k-\epsilon$ model. In the second case (comparison of CO concentration) the EARSM model predict lower concentration of CO emissions but the k epsilon capture better the shape of concentration profile.

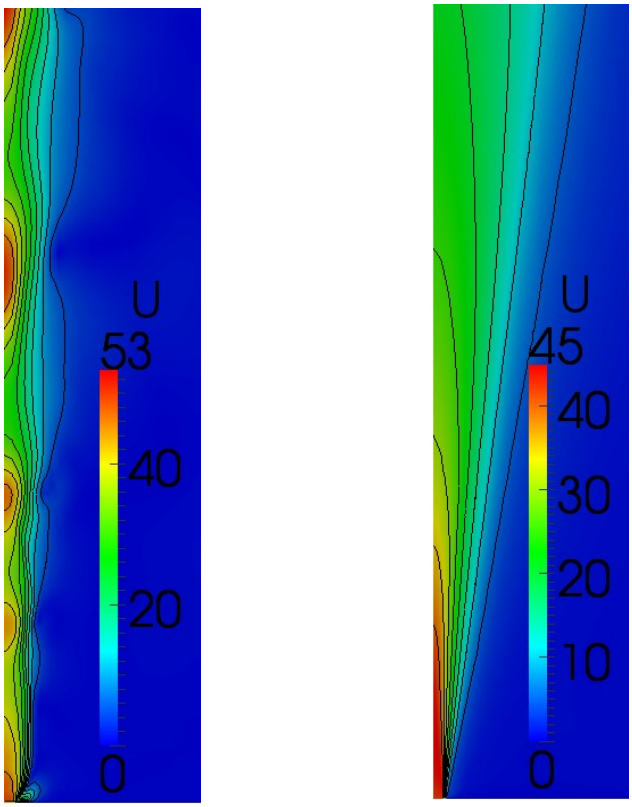

Figure 4: Sandia test case – Contours of velocity magnitude left $k-\epsilon$, right EARSM

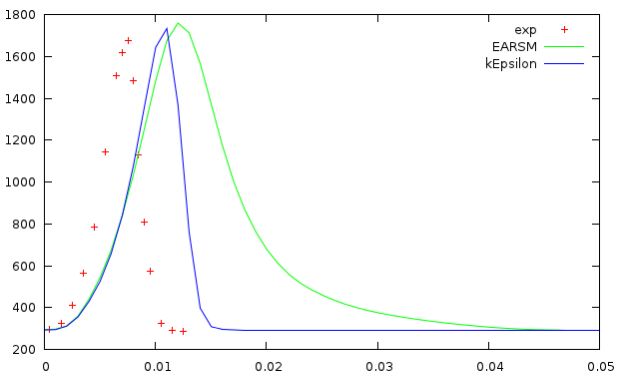

Figure 5: Sandia test case – Temperature profile x/d = 5

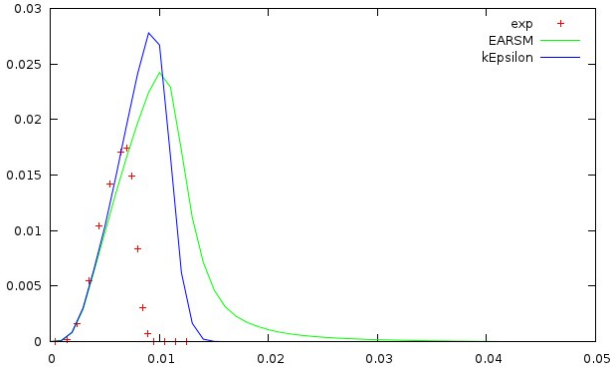

Figure 6: Sandia test case – CO concentration profile x/d = 5

One possible explanation for this phenomenon is simplification of terms for turbulent flux of heat and mass fraction (17) in EARSM turbulence model.

$$\overline{u_j h} \quad \text{and} \quad \overline{u_j Y_i} \tag{17}$$

These fluxes are simplified by isotropy turbulent viscosity

$$\overline{u_j h} = \frac{\mu_t}{Pr_t} \frac{\partial h}{\partial x_j} \quad , \tag{18}$$

$$\overline{u_j Y_i} = \mu_t \frac{\partial Y_i}{\partial x_j} \quad . \tag{19}$$

3.3 JETIS Combustion chamber

If EARSM turbulence model is applied to the flow modeling inside JETIS combustion chamber then several interesting differences, compared to older results, are observed. In the non-reacting case is a temperature increase near the fuel nozzle and closed to mixing zone. The temperature increase in the near of nozzle predict non-symmetric flow from delivery tubes into primary zone. The second increase of temperature is due the interaction of main flow from primary zone and jets of fresh air in mixing zone.

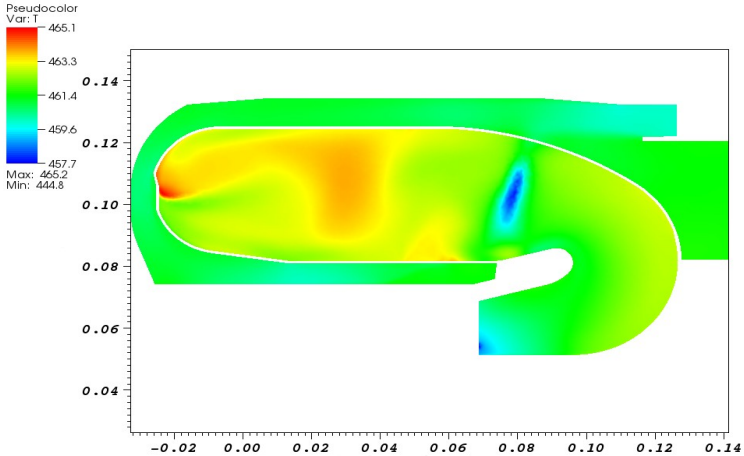

Figure 7: JETIS chamber – Temperature field non-reacting case

In Figure 8 is shown the L2 norm of anisotropy tensor. There is shown that the anisotropy maximum is in the mixing zone and in jets from delivery tubes.

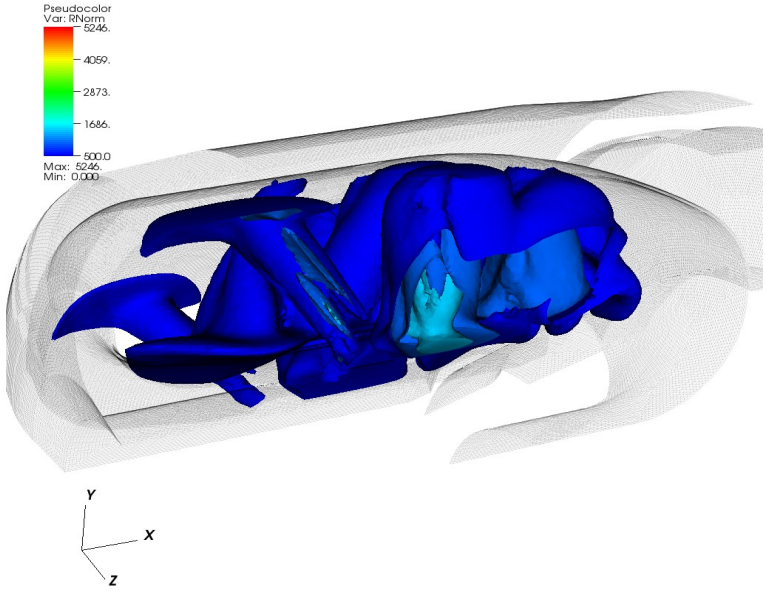

Figure 8: JETIS chamber – L2 norm of anisotropy tensor

The comparison of selected quantities for different types of turbulence model is shown in Table 1. There is quite good agreement between Low-Re models ($k-\omega$ *SST* , EARSM, LES) that improve especially prediction of pressure and densities.

Table 1: Comparison of selected quantities – nonreacting case

	$k-\omega$ *SST* HighRe	$k-\omega$ *SST* LowRe	EARSM	LES
Average inlet pressure [Pa]	508558	518354	519228	523472
Average outlet velocity [ms^{-1}]	79.49	79.8	79.64	78.1
Maximal density [kgm^{-3}]	3.87	3.94	3.99	4.2
Minimal density [kgm^{-3}]	3.24	3.18	3.12	3.14

Significant improvement of results have been observed in the case of reacting flow. As is shown in figures 9 and 10 or in table 2 the EARSM predict more realistic results than $k-\omega$ *SST* model. The maximum temperature(1700K) is concentrated in the case of EARSM model into primary zone. In the case of $k-\omega$ *SST* is temperature maximum(2273K) in the mixing and exhaust zone. This is due the wrong turbulent time scale determination. This is reflected to the average values on the outlet, where significant decrease in the case of EARSM model is shown.

Table 2: Comparison of selected quantities – reacting case

	$k-\omega$ *SST* HighRe	EARSM
Average outlet temperature [K]	1658.91	856.927
Average outlet CO concentration [-]	0.0004	0
Average outlet NO concentration [-]	0.013	0.009

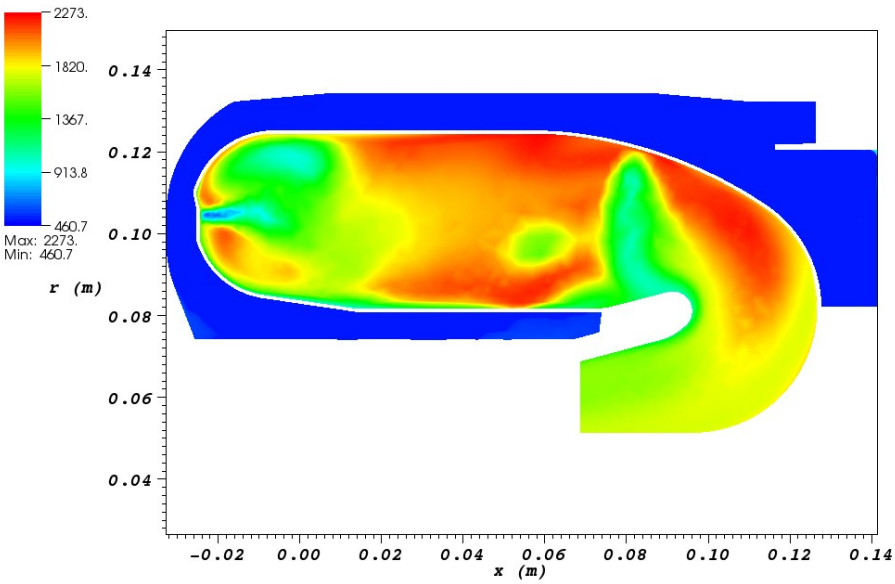

Figure 9: JETIS chamber – Temperature field reacting case $k-\omega$ *SST*

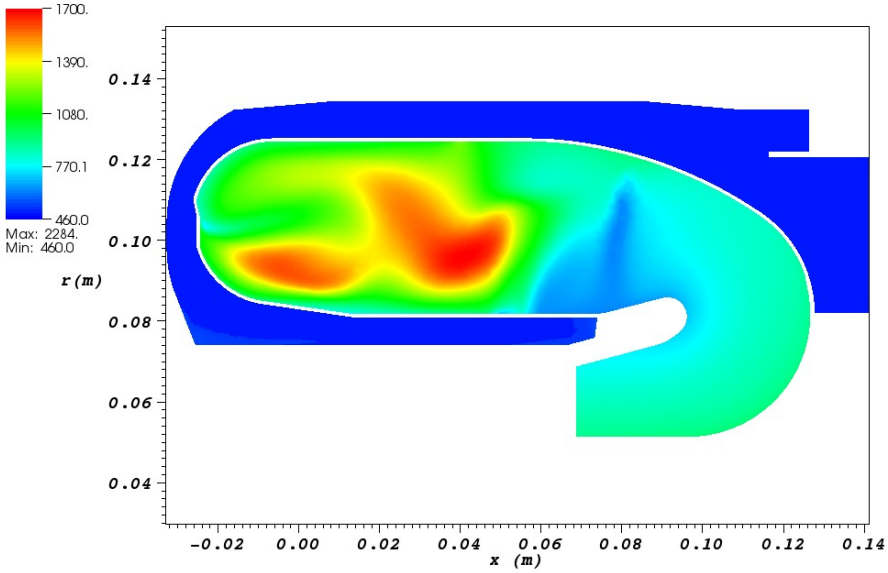

Figure 10: JETIS chamber – Temperature field reacting case EARSM

4 CONCLUSIONS

The application of EARSM turbulence model to the reacting flow field simulation was shown in this paper. This model provides many advantages(e.g. quality of results, computational stability, hardware and time requirements) and offers an interesting alternative to LES simulations. This should be a benefit for small industrial companies that used standard two equations RANS model in their simulations.

The EARSM model was used in original form presented by Hellsten in [5]. This form does not contain an algebraic expressions for anisotropic turbulent heat and mass fraction fluxes that allow the next improvement of results.

The future work will be oriented to improvement of EARSM turbulence model by algebraic expression for turbulent fluxes of heat and mass fractions, and to the test with developed multi-region solver for combustion simulation[8].

REFERENCES

[1] Betak, V., Kubata, J., Tuma, J. *Numerical simulation of liquid fuel combustion in the small aircraft combustion chamber*, *Czech Aerospace Proceedings*, (2010)

[2] Poinsot, T., Veynante, D. *Theoretical and Numerical Combustion*, Edwards, (2005)

[3] Durbin, P. A.: *Separated flow computations with the k-ε-v2 model*," *AIAA Journal*, vol. 33, no. 4, (1995)

[4] Wallin, S., Johansson, A.V. *Modelling streamline curvature effects in explicit algebraic Reynolds stress turbulence models*, *Int. J. Heat and Fluid Flow* (23),(2002)

[5] Hellsten, A.*New Two-Equation Turbulence Model for Aerodynamics Applications*, Espoo, Finland, 2004
[6] VKI Lecture Series *Turbulent Combustion Modeling, (*2011)
[7] Sandia TNF Workshop: *http://www.sandia.gov/TNF/DataArch/DLRflames.html*
[8] Betak, V. Simulation of reacting flow using splitted solver, NCAS, (2013)

ACKNOWLEDGMENT

This work was supported by the European Commission in the seventh framework program, grant No. ACP1-GA-2011-284859-ESPOSA.